Dalton Transactions

Accepted Manuscript

ROYAL SOCIETY OF CHEMISTRY

www.rsc.org/dalton

Dalton Transactions

RSCPublishing

ARTICLE

Synthesis, Structure and Valence-Trapping vs Detrapping for New Trinuclear Iron Pentafluoro benzoate Complexes: Possible Recognition of Organic Molecules by ^{57}Fe-Mössbauer Spectroscopy †

Cite this: DOI: 10.1039/x0xx00000x

Received 00thDecember 2013
Accepted 00th 2014

DOI: 10.1039/x0xx00000x

www.rsc.org/

Satoru Onaka,*[a,b] Yoichi Sakai,*[a] Tomoji Ozeki,[c] Tadahiro Nakamoto,[d] Yusuke Kobayashi,[c] Masashi Takahashi,[e] Ryo Ogiso,[a] Tsutomu Takayama,[a] Michito Shiotsuka[f]

New mixed-valence trinuclear iron pentafluorobenzoate complexes were synthesized. Their valence-detrapping and/or valence-trapping phenomena were studied by ^{57}Fe-Mössbauer spectroscopy and X-ray crystallography. For $[Fe_3O(C_6F_5CO_2)_6(py)_3]\cdot CH_2Cl_2$(**1**), a valence-trapped state was observed at low temperatures, while the valence-detrapped state was observed at room temperature. Removal of CH_2Cl_2 from **1** gives de-solvated $[Fe_3O(C_6F_5CO_2)_6(py)_3]$(**2**) where the valence was trapped at room temperature. The CH_2Cl_2-free **2** can reversibly absorb and desorb CH_3CN; the process was followed by ^{57}Fe-Mössbauer spectroscopy by monitoring valence-trapping and valence-detrapping phenomena. Organic molecules such as benzene, toluene, ethylbenzene, cumen, and xylene are also trapped by **2** and affect the iron valence states. However, small molecules such as H_2O and CO_2 do not affect the valence-trapped state of **2**. Three xylene isomers trapped within the nano-void of **2** were distinguished by ^{57}Fe-Mössbauer spectroscopy at room temperature.

Introduction

Since the structural elucidation of $[M_3O(CH_3CO_2)_6(H_2O)_3]Cl\cdot 2H_2O$ (M = Cr and Fe) in 1965[1], many carboxylate analogues of the form $[M_3O(RCO_2)_6L_3]^{+/0}$ (M = transition metal, L = ligand) have been synthesized and their magnetic and/or electronic behaviours have been studied extensively.[2,3] Among them, mixed-valence trinuclear iron derivatives（$M_3 = Fe^{III}{}_2Fe^{II}$） have attracted many chemists because of their interesting electron transfer behaviours in the solid state ; [4−10] ^{57}Fe-Mössbauer spectroscopy is a strong tool to study such a valence-trapping vs detrapping phenomenon. Hendrickson et al. have demonstrated that the solvent molecule plays an important role in determining the intramolecular electron transfer with a cooperative phase transition for a series of $[Fe_3O(CH_3CO_2)_6L_3](S)_n$ (L represents pyridine and/or its derivatives and S a solvent molecule).[6-10] Sorai et al. have verified the phase-transition in accord with a change from a valence-trapped state to a valence detrapped state by precise heat capacity measurements for $[Fe_3O(CH_3CO_2)_6(py)_3]\cdot py$; [11, 12] two phase transition temperatures at 111 K and 191.5 K among observed four phase transitions correspond to Mössbauer spectral changes caused by the change of an intramolecular electron transfer rate. They have also observed unexpected large entropy jumps at these phase transition temperature regions. Further explorations by use of heat capacity measurements and/or ^{2}H-NMR have shown that the solvent molecules should play an essential role in valence-detrapping via increasing intramolecular electron transfer rate, accompanied by the cooperative phase transitions induced by re-orientation movements of the solvent molecules for the series of $[Fe^{III}{}_2Fe^{II}O(CH_3CO_2)_6L_3]\cdot S$ complexes.[12] In addition, they have found that the valence-detrapping occurs at room temperature upon substitution of other solvent molecules for solvated pyridine in $[Fe^{III}{}_2Fe^{II}O(CH_3CO_2)_6(py)_3]\cdot py$.[6, 8] Nakamoto and Sano et al. have successfully synthesized a variety of new mixed-valence trinuclear iron carboxylate derivatives $[Fe_3O(RCO_2)_6L_3]$（L represents pyridine and/or H_2O）including long chain fatty acid anions, halogenoacetates, cyanoacetate, and/or pivalate instead of acetate with or without solvent molecules. They have verified for the first time that long alkyl chain can induce valence-detrapping in spite of the lack of a solvent molecule for $[Fe_3O(RCO_2)_6(py)_3]$ (RCO_2^- = myristic anion, palmitic anion, and stearic anion, respectively and L represents pyridine).[13] Powder X-ray patterns for these clusters exhibited layered structures and these long alkyl chains are supposed to play a similar role to those of solvent molecules for intramolecular electron transfer (electron hopping) demonstrated by Hendrickson et al.[13] They have also shown interesting results that an electronic dipole moment is produced from the electronically trapped Fe_3O molecule and the intermolecular dielectric interaction by this dipole moment plays a crucial role for valence-trapping vs valence-detrapping phenomena for the cyanoacetate derivative, $[Fe_3O(CH_2CNCO_2)_6(H_2O)_3]$.[14] They have found quite interesting results for halogenoacetate derivatives in which the partial valence-detrapping between one Fe^{III} site (Fe^{IIIA}) of two Fe^{III} ions and the Fe^{II} ion is observed with increasing temperature for $[Fe_3O(CH_2ClCO_2)_6(H_2O)_3]\cdot 3H_2O$ where intra- and inter-molecular hydrogen bonds are formed.[15] They have suggested that hydrogen-bonding interaction affects the local environment of iron atoms and induces valence delocalization between the two iron ions.[15] R. Wu et al. have reported soon after that similar partial valence-detrapping between one of the Fe^{III} sites and the Fe^{II} site is observed for $Fe_3O(Me_3CCO_2)_6(py)_3$ at low

temperatures.[16] C-C.Wu et al. have shown more complicated valence-detrapping phenomenon for $[Fe_3O(CH_3CO_2)_6(3\text{-Cl-py})_3]\cdot 3\text{-Cl-py}$, that is, the Fe^{II} signal splits into two doublets with raising temperature from 110 K.[9] They have interpreted this phenomenon in terms of the different disordered solvent environments. In spite of elaborated studies by Hendrickson et al. and Sano et al., there remains some issues to be explored further for the mechanism of valence-trapping and valence-detrapping.

We have supposed that the local valence-detrapping between one Fe^{III} site of two Fe^{III} ions and one Fe^{II} site may occur for molecules with lower symmetry than isosceles triangle without solvent molecules and/or without hydrogen bonds if such a mixed valence $[Fe_3O(RCO_2)_6L_3]$ complex is synthesized. In addition, mixed valence iron benzoate derivatives have not yet been reported so far to the best of our knowledge, although $[Fe^{III}{}_3O(PhCO_2)_6(py)_3]ClO_4\cdot py$ has been synthesized in 2001.[17] One of us (S.O.) has also reported the synthesis of mixed valence manganese analogous $[Mn_3O(C_6F_5CO_2)_6(py)_3]\cdot x(CH_2Cl_2)$ (x = 0 or 1) in 2003.[18] In this paper, we will report successful synthesis of new pentafluorobenzoate derivatives $[Fe^{III}{}_2Fe^{II}O(C_6F_5CO_2)L_3]\cdot x(CH_2Cl_2)$ (x = 0 or 1 and L represents py), X-ray structure analysis, and ^{57}Fe-Mössbauer spectroscopic studies on valence-trapping vs valence-detrapping. We will also suggest possible recognition of organic molecules by ^{57}Fe-Mössbauer spectroscopy.

Results and Discussion

Synthesis

A new $Fe^{III}{}_2Fe^{II}O(C_6F_5CO_2)_6L_3\cdot xS$ (x = 1;L = py; S = CH_2Cl_2) (**1**) complex has been synthesized in ethanol at ambient temperature with moderate yield according to the following equation.

$$2FeCl_3 + FeCl_2 + 6C_6F_5CO_2Na + L(\text{excess}) \rightarrow Fe^{III}{}_2Fe^{II}O(C_6F_5CO_2)_6L_3\cdot xS \quad (1)$$

This is a typical carboxylate-metal cluster with bridging benzoate ligands and three pyridine ligands.[18,19] TG-MS measurement of **1** exhibits a step of one CH_2Cl_2 molecule loss upon heating in the range from 100 to 160 ℃ and the resulting "solvent-free cluster **2**" is stable up to 200 ℃ (Fig. S1, ESI); the species lost during this step was confirmed to be CH_2Cl_2 by MS. Powdered sample of **1** does not absorb any CH_2Cl_2 more. The preliminary paper has been reported elsewhere.[19] We are tempted to examine that **2** may behave as a porous material like pyrazin-2-carboxylate Zn derivatives to trap medium-size molecules such as methanol and/or ethanol.[20] Quite interesting chemical behaviours of **2** to organic molecules are described in the Mössbauer section.

X-ray Structure Analysis

The molecular structure of **1** is shown in Fig. 1. Complex **1** crystallizes in a hexagonal space group $P6_3/m$. The central oxygen atom O1 is located at a crystallographic C_{3h} position in **1**. Therefore, three Fe atoms are equivalent, which is consistent with the Mössbauer data that two Fe^{III} and one Fe^{II} atoms are in a valence-detrapped state at room temperature. The observed Fe-O1 distance, 1.9088(4) Å is just between typical Fe^{III}-O distances (1.85 to 1.89 Å) and typical Fe^{II}-O distances (1.93 to 2.01 Å).[3, 6-16] Slight differences are observed for Fe-carboxylate O distances (2.0569(14) and 2.0674(14) Å). Three pyridine rings are perpendicular to the mirror plane which contains three Fe atoms and the central O atom.

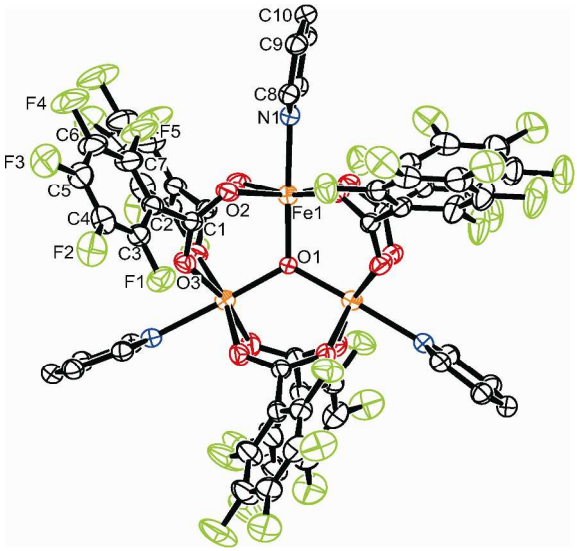

Fig.1. Molecular structure of **1**.

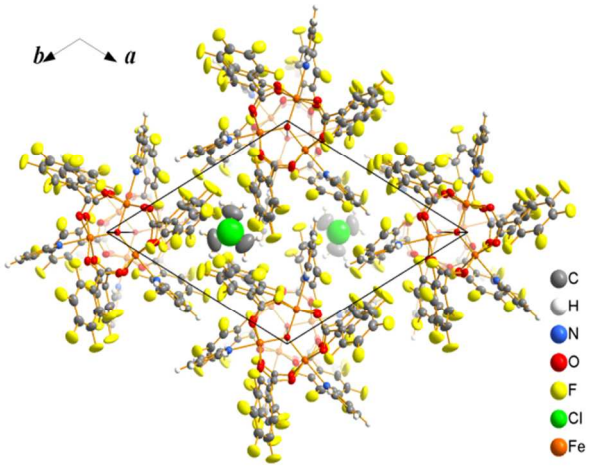

Fig.2. Packing diagram of **1** viewed along the *c*-axis.

Figure 2 shows a packing diagram of **1** viewed along the *c* axis. Guest CH_2Cl_2 molecules are located in nano-voids which are formed by C_6F_5 rings and pyridine rings from neighboring Fe_3 clusters. The distances among H atoms in CH_2Cl_2 and F atoms in C_6F_5 rings are longer than those of typical hydrogen bonds. The guest CH_2Cl_2 molecules are very likely to be kept in the void by van der Waals force. The specimen used for the single crystal X-ray diffraction seems to have lost some portion of its solvent of crystallization and is best refined as a 0.735 CH_2Cl_2 solvated complex. The crystal structure of **1** is quite similar to the manganese analogue of $Mn_3O(C_6F_5CO_2)_6(py)_3$, which totally lacks solvent CH_2Cl_2 molecules and belongs to the hexagonal space group $P6_3/m$ suggesting this Mn_3O complex is in the valence detrapped state similar to **1**.[18,21]

^{57}Fe Mössbauer Spectra

The temperature-dependent Mössbauer spectra of $Fe_3O(C_6F_5CO_2)_6(py)_3\cdot CH_2Cl_2$ (**1**) are shown in Fig. 3. Mössbauer parameters are summarized in Table 1.

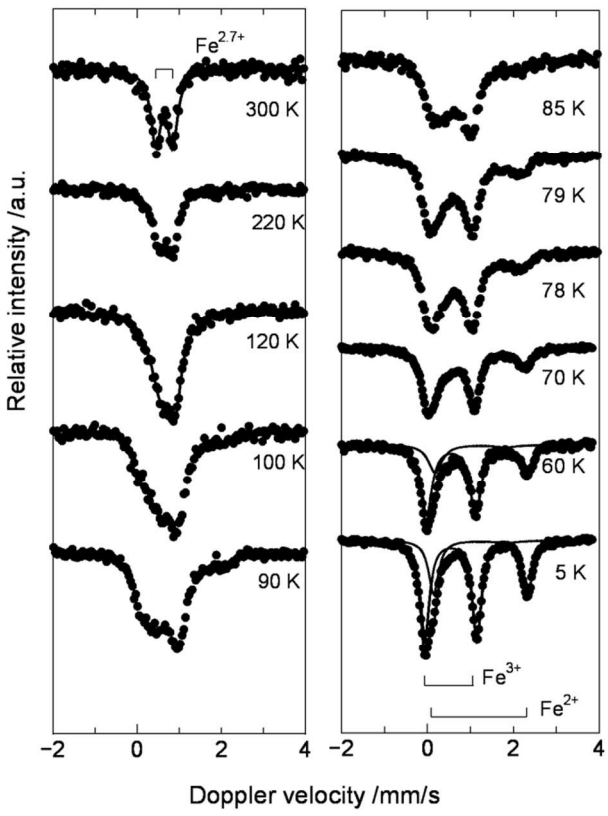

Fig.3. ^{57}Fe Mössbauer spectra of $[Fe_3O(C_6F_5CO_2)_6(py)_3]\cdot CH_2Cl_2$ (**1**)

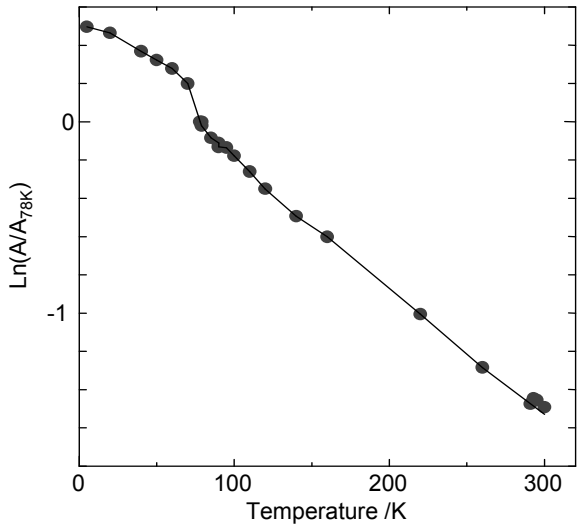

Fig.4. A plot of Mössbauer absorption total area intensities, *A* vs temperatures for **1**.

Two sets of quadrupole-split doublets are observed at very low temperatures with the area ratio of 1:2, which are assigned to high-spin Fe^{II} and high-spin Fe^{III} sites, respectively; valence is trapped in the low temperature regions. The two quadrupole-split doublets become indistinguishable and then coalesce into one quadrupole-split doublet at room temperature, showing an intermediate isomer shift value of Fe^{II} and Fe^{III} ions, that is, $Fe^{2.7+}$. It is difficult to determine the exact transition temperature from the valence-trapped state to valence-detrapped state on the basis of temperature-dependent Mössbauer spectra. Figure 4 shows plots of Mössbauer absorption total area intensities, *A* of these two pairs of doublets vs temperatures; in the high temperature approximation of the Debye model, temperature dependence of *A* can be expressed in the form

$$d(\ln A)/dT = -3E_\gamma^2/Mc^2k\theta^2 \quad (2)$$

where E_γ is the Mössbauer transition energy, *M* the effective mass imparted the recoil energy by emission of the Mössbauer γ-ray, θ the Debye temperature, *c* the velocity of light, and *k* the Boltzmann constant. In the right-hand of Equation (2), the unknown physical quantities characteristic to this chemical matter is *M* and θ, which cannot be evaluated independently in the present analysis, just giving the product $M\theta^2$. The quantity of $M\theta^2$, obtained as $-3E_\gamma^2/c^2k$ (the slope of the plot), is called "intermolecular force constant" by Matsubara et al.,[22] both the *M* and θ quantities being correlated positively to the rigidity of solids. The slope of the plots is inversely proportional to $M\theta^2$ and is discontinuous at around 80 K (for below and above 80 K, the $M\theta^2$ values were estimated $2.51(14) \times 10^{-21}$ and $1.92(3) \times 10^{-21}$ kgK^2, respectively), being consistent with the observation (Fig. 3) that the valence-trapped state has begun to change to the valence-detrapped state around this temperature for **1**. Assuming that the effective mass *M* is that of one molecule of the complex, the Debye temperatures θ were calculated to be 30 K (below 80 K) and 26 K (above 80 K) with or without a solvated molecule.[23] Upon the loss of solvent CH_2Cl_2 from **1**, the Mössbauer spectra change drastically for **2** as shown in Fig.5; the valence is trapped even at room temperature. Hendrickson et al. have reported that the solvent molecule plays an important role in valence-detrapping and valence-trapping phenomena for a series of $Fe_3O(CH_3CO_2)_6L_3\cdot xS$ ($x = 0$ or 1).[6-10]

^{57}Fe Mössbauer Spectroscopic Study on Absorptions of Organic Molecule Vapour by 2

In the previous paper, we have reported that the solvent CH_2Cl_2 is reversibly lost and absorbed for the manganese analogue of $Mn_3O(C_6F_5CO_2)_6(py)_3\cdot CH_2Cl_2$.[18,21] Single crystal x-ray analyses have shown that **1** and CH_2Cl_2 desolvated manganese-analogue $Mn_3O(C_6F_5CO_2)_6(py)_3$ are isomorphous.[18,21] A channel-like structure is found in **1** as shown in Fig.2. CH_2Cl_2-free $Mn_3O(C_6F_5CO_2)(py)_3$ has a similar channel structure. Therefore, we are tempted to explore CH_2Cl_2 de-solvation and solvation phenomenon for **1** at first; one molecule of CH_2Cl_2 is easily lost from **1** as described in the synthetic section. Vapour-trap experiments for **2** were done for CH_2Cl_2 in a double vial apparatus as described below. Approximately 100 mg sample of **2** was placed in a small size vial and then this vial was placed in a large size vial. A little amount of CH_2Cl_2 was poured in the large vial and the large vial was capped. The weight increase of **2** after exposing to CH_2Cl_2 vapour for several hours corresponds to one molecule of CH_2Cl_2, indicating restoration of **1** (Fig. 6). The $\mathbf{2}\cdot CH_2Cl_2$ complex shows valence-trapped Mössbauer spectra at low temperatures, while a valence-detrapped spectrum is observed at room temperature; the spectra for the restored sample are indistinguishable from that of **1** over the measured temperature region (78-294 K). These Mössbauer spectral changes also strongly support that the CH_2Cl_2 adduct of **2** is **1**. We imagined that organic molecules with similar size to CH_2Cl_2 would be trapped in the void of **2**. In order to explore the possibility of **2** as

Dalton Transactions RSCPublishing

ARTICLE

Table 1. ^{57}Fe Mössbauer Parameters for **1** and **2**.

	$[Fe_3O(C_6F_5CO_2)_6(py)_3]\cdot CH_2Cl_2$ (**1**)											
	δ (mm/s)			ΔE_Q(mm/s)			Γ (mm/s)			area(%)		
T/K	Fe^{III}	Fe(av)	Fe^{II}	Fe^{III}	Fe(av)	Fe^{II}	Fe^{III}	Fe(av)	Fe^{II}	Fe^{III}	Fe(av)	Fe^{II}
300		0.640(5)			0.401(8)			0.248(12)			100	
220		0.685(5)			0.322(7)			0.329(12)			100	
120		0.724(5)			0.331(10)			0.502(16)			100	
60	0.549(2)		1.247(5)	1.139(4)		2.140(10)	0.308(6)		0.382(17)	67(1)		33(1)
5	0.544(1)		1.234(2)	1.210(1)		2.186(3)	0.257(2)		0.283(4)	62(1)		38(1)

	$[Fe_3O(C_6F_5CO_2)_6(py)_3]$ (**2**)							
	δ (mm/s)		ΔE_Q(mm/s)		Γ (mm/s)		area(%)	
T/K	Fe^{III}	Fe^{II}	Fe^{III}	Fe^{II}	Fe^{III}	Fe^{II}	Fe^{III}	Fe^{II}
300	0.434(3)	1.115(11)	1.250(5)	1.243(22)	0.291(9)	0.428(28)	65(2)	35(2)
270	0.452(3)	1.172(10)	1.272(5)	1.362(19)	0.322(9)	0.420(25)	66(2)	34(2)
230	0.473(2)	1.179(7)	1.286(5)	1.401(15)	0.307(8)	0.374(21)	68(2)	32(2)
190	0.492(2)	1.236(7)	1.297(6)	1.514(13)	0.342(9)	0.351(20)	68(2)	32(2)
160	0.504(2)	1.235(4)	1.297(4)	1.562(9)	0.316(6)	0.345(13)	67(1)	33(1)
120	0.521(3)	1.263(5)	1.278(5)	1.641(10)	0.353(8)	0.330(15)	67(2)	33(1)
78	0.529(2)	1.273(5)	1.292(4)	1.816(9)	0.318(5)	0.374(13)	65(1)	35(1)

Isomer shifts (δ mm/s) refer to α -iron; ⊿E_Q＝quadrupole splitting (mm/s), Γ = full width at half maximum of the Lorentzian lines (mm/s). Statistical standard deviations are given in parentheses, estimated from fitting procedure using the MossWinn 4.0 Pre software.

a nano-porous material, the similar procedure as described above was employed for several organic vapour. Powder sample of **2** (a few-ten mg to 100 mg) was used and a little amount of organic liquid is poured in the large vial for each exposure experiment. The total pressure inside the larger vial is the sum of the atmospheric pressure of the air and the saturated vapour pressure of organic molecule. The exposed periods were ranged from 12 minutes to several-tens of hours. Acetonitrile was used at first to examine our idea. As shown in Fig.S2c (ESI), the valence-trapped state of **2** is changed to the valence-detrapped state at room temperature after exposure to CH_3CN. The weight increase plot against exposure time is quite similar to **2**·CH_2Cl_2. The product with a tentative formula **2**·CH_3CN was heated under a reduced pressure to ascertain that CH_3CN could be removed from the complex. The spectrum of **2** is regained after this treatment as is illustrated in Fig. S2d (ESI); spectral shape resembles that of **2** (Fig. S2b,,ESI), suggesting that **2**·CH_3CN is almost returned to **2**. This finding suggests that other organic molecules would be incorporated in an intermolecular nano-void of **2**. Mössbauer spectral measurements of **2** after exposure to vapour of several organic molecules were done at room temperature; similar spectral changes to **2**·CH_3CN were observed for benzene, toluene, ethylbenzene, and cumene, as illustrated in Fg. 7. Carbon tetrachloride, chloroform, THF, and ethanol exhibited similar spectral changes (spectra for these molecules were not shown). Such a spectral change, however, was not observed for H_2O and CO_2; examined samples are exposed subsequently to CH_3CN vapour, resulting in a detrapped-type spectrum. It is concluded from this observation that H_2O and CO_2 cannot be kept in the intermolecular nano-voids of **2** or the interaction of these small molecules with host nano-channels of **2** are too weak to be detected by Mössbauer spectroscopy at room temperature. Organic

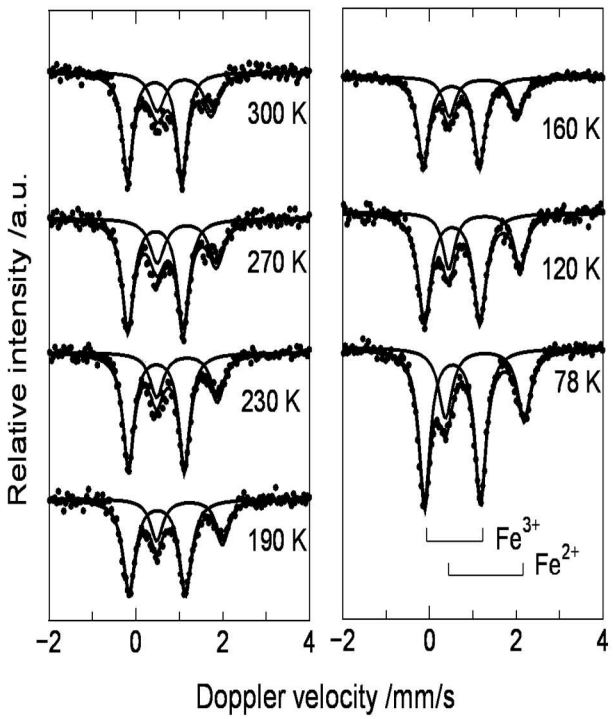

Fig.5. ^{57}Fe Mössbauer spectra of $[Fe_3O(C_6F_5CO_2)_6(py)_3]$ (**2**)

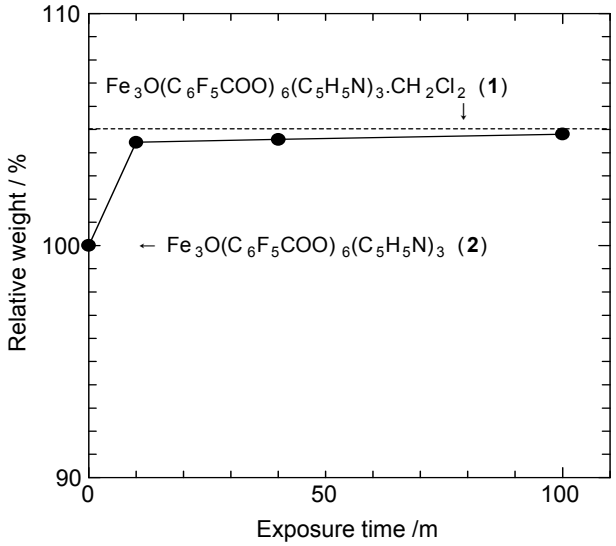

Fig.6. A plot of weight increase of **2** by absorbing CH_2Cl_2 at room temperature.

molecules mentioned above may be easily trapped in hydrophobic environments and/or channels which are yielded by C_6F_5 rings and pyridine rings in **2**. Our finding that even $C_6H_5CH_3$ and $C_6H_5CH(CH_3)_2$ are trapped in the nano-voids leads to further exploration into recognition of xylene isomers, the size of which are close to those of toluene and cumene. As shown in Fig. 8, three xylene isomers afford clearly different Mössbauer spectra to one another's at room temperature. Mössbauer spectra at 78 K for these three adducts look like that of **1** in the valence-trapped state (Fig. 9), although completely valence-trapped states are expected below 78 K. The supposed complex **2**·*o*-xylene shows a quite similar Mössbauer spectrum to that of **1** at room temperature indicating the valence-detrapped state. The Mössbauer spectrum of supposed complex **2**·*m*-xylene at room temperature resembles that of **1** at 100 K and the Mössbauer spectrum of supposed complex **2**·*p*-xylene at room temperature resemble that of **1** at 85 K. These two are transient spectra from valence-trapped to valence-detrapped states. Thus transition temperatures from valence-trapped state to valence-detrapped state for xylene adducts of **2** are estimated in the order *o*-xylene <*m*-xylene <*p*-xylene. This order strongly suggests that the shape and/or the size of nano-void are influenced by guest xylene isomers and xylene isomers play an essential role for determining the electron hopping rate in xylene addcuts of **2**; xylene molecules should play a similar role for determining an electron hopping among the Fe_3 triangle to the case of $Fe_3O(CH_3CO_2)_6(py)_3.py$.[6,] This is the first report that the xylene isomers are distinguished by Mössbauer spectroscopy to the best of our knowledge. For furthe exploration how xylene isomers are distinguished by ^{57}Fe-Mössbauer spectroscopy, weight increases of **2** upon exposure to xylene vapour were examined. The observed weight increase for each xylene isomer is almost consistent with that of 1:1 adduct formation as in the case of CH_2Cl_2. Figure 10 shows powder X-ray diffraction (XRD) patterns of **1**, **2**, and organic molecule adducts of **2** mentioned above. Observed XRD pattern of **1** is in coincidence with that of the calculated one by Mercury 2.3 program based on the single crystal diffraction data, while that of **2** is different from that of **1**, indicating that **2** belongs to a different space group from $P6_3/m$. XRD patterns of 1:1 adducts of **2** with aromatic molecules such as benzene, toluene, ethylbenzene, cumene, and xylene isomers are quite similar to that of **1** except the *p*-xylene adduct, indicating that **1** and these adducts are isomorphous, although lattice constants are little bit changed depending on the size of organic molecules incorporated in nano-voids of **2**; detailed analysis of lattice changes by guest molecules will be discussed in a forthcoming paper. Observed similarity in XRD patterns of adducts of **2** leads to a conclusion that two organic molecules occupy the same sites of CH_2Cl_2 in **1** in the unit cell. However, the observed XRD pattern of *p*-xylene adduct of **2** is neither similar to that of **1** nor that of **2**.The shape of nano-channel and/or the nano-structure of **1** and/or **2** is expected to be more flexible than those of designed nano-architectures described in literatures,[20,24-27] because the nano-architecture is composed from C_6F_5 and pyridine rings; the characteristic of nano-architectures in **1** and/or **2** is its "softness or flexibility". This feature presumably enables accommodations of various sizes of organic molecules. The longest *p*-xylene among the examined organic molecules, however, forces significant deformation of the nano-structures and/or the unit cell dimensions of *p*-xylene adduct of **2** from the original nano-structure of **1** by trapping *p*-xylene molecule in **2** leading to another space group. Temperature-dependent ^{57}Fe Mössbauer spectral behaviours for *o*- and *m*-xylene isomers are interpreted in terms of similar contribution of the solvent molecule motions to that of $[Fe_3O(CH_3CO_2)_6(py)_3]\cdot py$.[11,12] However, interpretation of temperature-dependent ^{57}Fe Mössbauer spectral changes for *p*-xylene adduct requests other factors than molecule motions of trapped *p*-xylene. The observed XRD pattern for the *p*-xylene adduct of **2** strongly suggests that the space group is different from $P6_3/m$. Contribution of other factors than enthropy changes by trapped *p*-xylene molecule motion to electron hopping is thus expected significantly different from other organic molecules employed in the present organic vapour exposure. The "soft nano-voids" in **2** thereby tempts us to explore an important new aspect of "soft nano-materials"

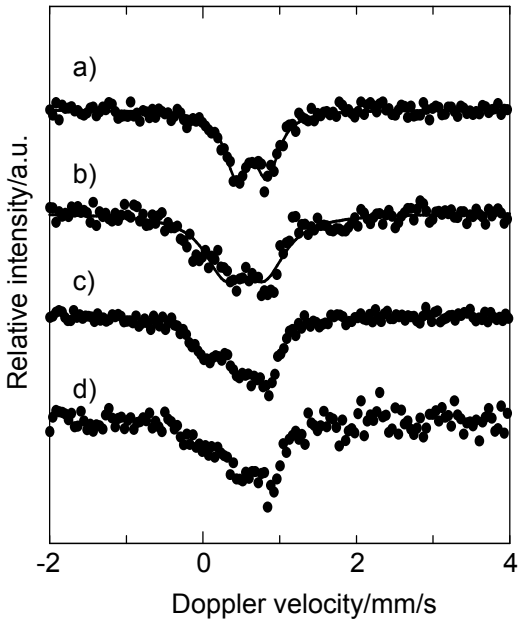

Fig.7. ^{57}Fe Mössbauer spectra of $Fe^{III}_2Fe^{II}O(C_6F_5COO)_6(py)_3$(**2**) exposed to organic vapour at room temperature; a), C_6H_6 vapour for 15 h; b), $C_6H_5CH_3$ vapour for 19 h; c), $C_6H_5C_2H_5$ vapour for 39h; d), $C_6H_5CH(CH_3)_2$ vapour for 20h.

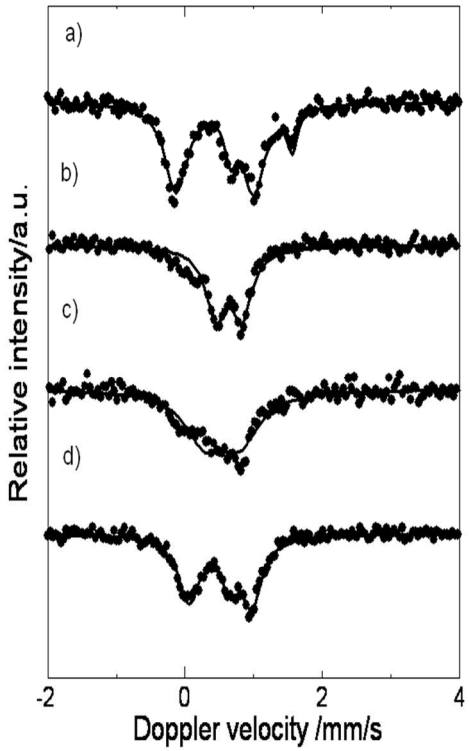

Fig.8. Room temperature Mössbauer spectra of $Fe^{III}_2Fe^{II}O(C_6F_5COO)_6(py)_3$ (**2**) exposed to xylene isomer vapour; a):**2**; b): *o*-xylene; c): *m*-xylene; d): *p*-xylene.

in addition to well-known "flexible supra-molecular nano-architectures".[20, 24-27]

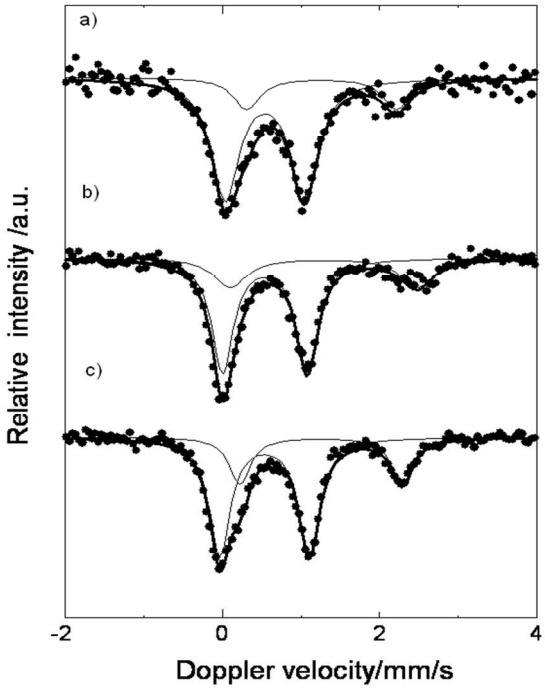

Fig.9. ^{57}Fe Mössbauer spectra of xylene adducts of **2** at 78 K; a):*o*-xylene adduct; b): *m*-xylene adduct; c): *p*-xylene adduct.

It is worthwhile to describe results of comparisons of IR spectra of **1** and **2** and **2** and CH_3CN adduct of **2** in the 4000-400 cm^{-1} region; any distinct changes were not detected for these pairs by an ordinary IR measurement. ^{57}Fe-Mössbauer spectroscopy is thus concluded to be quite sensitive and indispensable technique to study organic molecule absorption vs desorption phenomena for trinuclear iron pentafluorobenzoate complexes.

Experimental

Materialsand general procedures

$C_6F_5CO_2H$ (Aldrich) was dissolved into a small amount of hot water and then neutralized by adding Na_2CO_3. Large portion of water was evaporated and most remaining water was taken off from the slurry by air-blowing while hot. The residue was dried on filter paper by standing at room temperature. IR spectra were recorded with a JASCO FT-IR-4200 spectrometer for Nujol mull samples in the range 4000-400 cm^{-1} at room temperature. TG-MS spectra were measured using a thermogravimetric analyzer (ShimadzuTG-40) coupled with a quadrupole mass spectrometer (Shimadzu GCMS QP2010) connected by an in-hose developed interface. Powder X-ray diffractions were measured by a Rigaku Geigerflex RAD-2C diffractometer (Cu K_α) at room temperature.

Synthesis

$[Fe_3O(C_6F_5CO_2)_6(py)_3]\cdot CH_2Cl_2$ (**1**). $FeCl_3.6H_2O$ (1.08 g, 4 mmol) and $FeCl_2.4H_2O$ (0.4 g, 2 mmol) were dissolved in 30 mL of ethanol by stirring. Then 4.8 mL of pyridine was added and the resulting orange-brown suspension was stirred for 10 min. To this was added $C_6F_5CO_2Na$ (2.92 g, 12.5 mmol) and the mixture was stirred for 2 h to afford almost black suspension. Black-brown precipitates were

Dalton Transactions RSCPublishing

ARTICLE

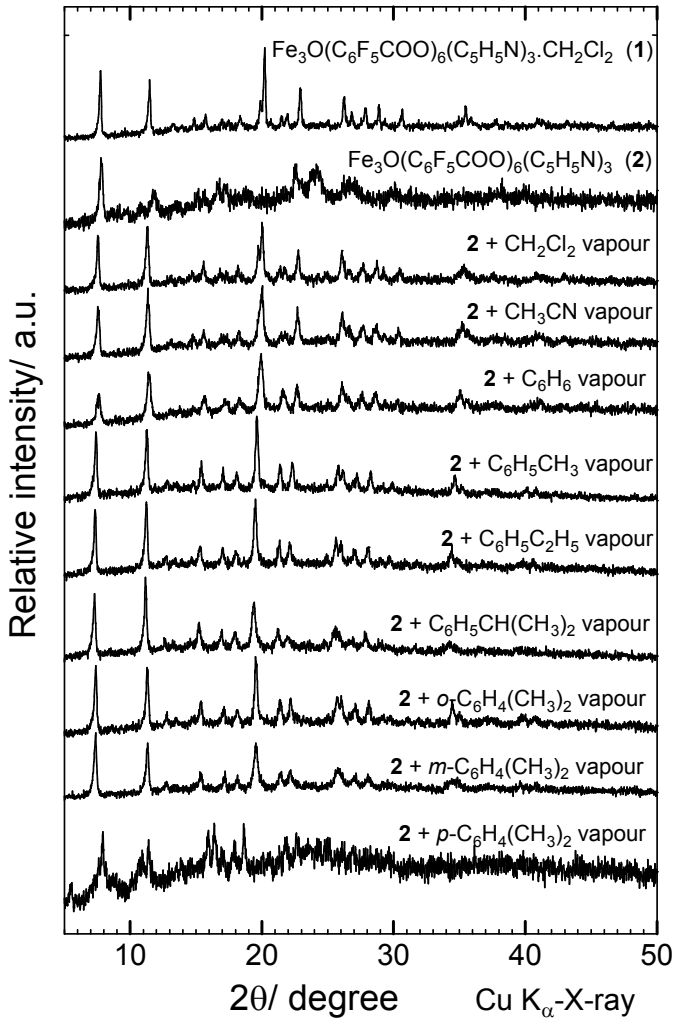

Fig. 10. Powder X-ray diffractions for **1**, **2**, and organic molecule adducts of **2** after exposure for 21 h at room temperature.

collected on filter-paper and the residue was extracted with each 20 mL of CH_2Cl_2 more than ten times until almost white solid was left on filter paper. Combined CH_2Cl_2 extracts were reduced to approximately 1/4 volume by evaporation of CH_2Cl_2 under a reduced pressure. Ethanol (10 mL) was added and 5 mL of hexane was layered over the solution. The mixture was stored in a refrigerator for several days to afford dark-brown needle-like crystals (2.13 g, yield 30 %). Anal. Calc. for $C_{57}H_{15}F_{30}Fe_3N_3O_{13}.CH_2Cl_2$:C,39.31;H, 0.97; N,2.37; F, 32.16; Cl, 4.00. Found: C, 39.81; H, 1.04; N, 2.43; F, 32.41; Cl, 3.09 %. TG-MS analysis indicates that one CH_2Cl_2 molecule is contained in **1**.[27] IR(Nujol):ν(CO)$_{asym}$; 1654(vs), 1636(s), 1606(m)cm^{-1}; ν(CO)$_{sy}$:1401(s)

$[Fe_3O(C_6F_5CO_2)_6(py)_3]$(2). A 178.5 mg ground sample of **1** was placed in a 10 mL volume flask and this flask was heated at about 130 ℃ (oil-bath) for 1.5 h under a reduced pressure (0.1 Torr). These experimental conditions were determined on the basis of TG-MS data for **1**. Observed weight loss was about 4.4 %, which was in good agreement with the loss of one CH_2Cl_2 molecule. Anal. Calcd for $C_{57}F_{30}Fe_3H_{15}N_3O_{13}$: C, 40.57; H, 0.90; N, 2.49;F,33.78. Found: C39.90; H, 0.88; N, 2.38;F, 34.30. IR(Nujol):ν(CO)$_{asym}$; 1654(vs), 1636(s), 1606(m) cm^{-1}; ν(CO)$_{sym}$; 1404(s)

^{57}Fe Mössbauer Spectroscopy

Mössbauer measurements were performed in an ordinary mode with a Mössbauer spectrometers (Topologic Systems Inc. for 77-300 K and WissEI 260A system for 5-70 K) with ^{57}Co(Rh) sources. Crashed but not ground crystals were used for measurements. Examined temperatures were ranged from 5 K to 300 K and/or from 78 K to 300 K. The spectral curve fitting was carried out by using Moss Winn 4.0 Pre (http://www.mosswinn.com/). The isomer shift and Doppler velocity scale were calibrated by the six lines of a body centered cubic iron foil (α-Fe), the center of which was taken as zero isomer shift.

X-ray Structure Analysis.

Single crystal X-ray data for **1** were collected by a Rigaku Mercury CCD diffractometer with a graphite monochromated Mo K_α radiation (λ = 0.71073 Å) at 123 K. Structures were solved by SIR92[29] and were refined by the full-matrix least-squares method.[30] All nonhydrogen atoms were refined with anisotropic displacement parameters while the hydrogen atoms were refined with a riding model. The molecular structure (Fig.1) and the crystal packing diagram for **1** (Fig.2) are drawn by ORTEP for Windows[31] and Diamond 3.2i.[32] Crystal data for **1**: $C_{57}H_{15}F_{30}Fe_3N_3O_{13}\cdot0.735CH_2Cl_2$, M = 1749.7, hexagonal, $P6_3/m$, a = 13.458(1), c = 20.967(1) Å, V = 3288.7(5) Å^3, T = 123(2) K, Z = 2, μ(Mo K_α) = 0.862 mm^{-1}. 15970 reflections were measured, of which 2775 were independent (R_{int} = 0.0408). The final $R1$ = 0.0439 for 2114 reflections with $I > 2\sigma(I)$ and $wR(F^2)$ = 0.1349 for all data.

CCDC reference number 975326 for **1** .

See http://dx.doi.org/ for crystallographic data in CIF or other electronic format.

Conclusion

New mixed-valence tri-iron pentafluorobenzoate complexes have been synthesized. Iron valences are detrapped for CH_2Cl_2-solvated **1**, while valences are trapped for CH_2Cl_2-free **2** at room temperature. Solvent-free **2** behaves as a nano-porous material and absorbs many kinds of organic molecule vapour. These behaviours including valence-trapping and/or valence-detrapping have been studied by ^{57}Fe-Mössbauer spectroscopy. Three xylene isomers have been recognized by ^{57}Fe-Mössbauer spectroscopy for the first time.

†Electronic supplementary information (ESI) available: See DOI:

Notes and references

[a]*Department of Chemistry, Daido University, Takiharu-cho, Minami-ku,Nagoya,457-8530,Japan,* [b]*Department of Environmental Technology, Graduate School of Engineering, Nagoya Institute of Technology, Gokiso-cho, Showa-ku, Nagoya 466-8555,Japan,* [c]*Department of Chemistry and Materials Science, Tokyo Institute of Technology, O-okayama,Megro-ku, Tokyo, 152-8551,japan,* [d]*Toray Research.Center,Ohtsu 520-8567, Japan,* [e]*Department of Chemistry, Toho University,Miyama, Funahashi, Chiba,274-8510, Japn*[f]*Department of Socio Science and Engineering, Graduate School of Engineering, Nagoya Institute of Technology, Gokiso-cho, Showa-ku, Nagoya 466-8555,Japan*

*Corresponding author (S.O). Emeritus Professor of Nagoya Institute of Technology, *E-mail*:onakaau19@se.starcat.ne.jp, *Corresponding author (Y. S). Daido University,*E-mail*: yocsakai@daido-it.ac.jp

1 B. N. Figgis, B. B. Robertson, *Nature*, **1965**, *205*, 694.
2 J. Catterick; P. Thornton, *Adv. Inorg. Chem. Radiochem*, **1977**, *20*,291.
3 R. D. Canon, R. P. White, *Prog. Inorg. Chem*., **1988**, *36*, 195.
4 D. Lupu, D. Barb, G. Filoti, M. Morariu, D. Tarina, *J. Inorg. Nucl. Chem*., **1972**, *34*, 2803.
5 C. Z. Dziobkwski, J. T. Wrobleski, D. B. Brown, *Inorg. Chem*., **1981**, *20*, 679.
6 S. M. Oh, D. N. Hendrickson, K. L. Hassett, R. E. Davis, *J. Am. Chem. Soc*., **1985**, *107*, 8009.
7 S. E. Woehler, R. J. Wittebort, S. M. Oh, T. Kambara, D. N. Hendrickson, D. Inniss, C. E. Strouse, *J. Am. Chem. Soc*., **1987**, *109*, 1063.
8 S. M. Oh, S. R. Wilson, D. N. Hendrickson, S. E. Woehler, R. J. Wittebort, D. Inniss, C. E. Strouse, *J. Am. Chem. Soc*., **1987**, *109*, 1073.
9 Chi-Cheng Wu, S. A. Hunt, P. K. Gantzel P. Gűtlich, D. N. Hendrickson, *Inorg. Chem*., **1997**, *36*, 4717.
10 S. M. Oh, T. Kambara, D. N. Hendrickson, M. Sorai, K. Kaji, S. E. Woehler, R. J. Wittebort, *J. Am. Chem. Soc*., **1985**, *107*, 5540.
11 M. Sorai, K. Kaji, D. N. Hendrickson, S. M. Oh, *J. Am.Chem. Soc*., **1986**, *108*, 702.
12 H. G. Jang, S. J. Geib, Y. Kaneko, M. Nakano, M. Sorai, A. L. Rheingold, B. Montez, D. N. Hendrickson, *J. Am. Chem. Soc*., **1989**, *111*, 173;Y. Kaneko, M. Nakano, M. Sorai, H. G. Jang, D. N. Hendrickson, *Inorg. Chem*., **1989**, *28*, 1067;S. E. Woehler, R. J. Wittebort, S. M. Oh, D. N. Hendrickson, D. Inniss, C. E. Strouse, *J. Am. Chem. Soc*., **1986**, *108*, 2938; H. G. Jang, R. J. Wittebort, M. Sorai, Y. Kaneko, M. Nakano, D. N. Hendrickson, D. N. Hendrickson, *Inorg. Chem*., **1992**, *31*, 2265 .
13T. Nakamoto, M. Katada, H.Sano, *Chem. Lett.*, **1990**, 225; T. Nakamoto, M. Katada, H.Sano, *Chem. Lett.*, **1991**, 1323; T. Nakamoto, M. Katada, H. Sano, *Inorg. Chim. Acta*, **1999**, *291*, 127.
14 T. Nakamoto, M. Katada, S. Kawata, S. Kitagawa, K. Kikuchi, I. Ikemoto, K. Endo, H. Sano,*Chem,Lett*., **1993**, 1463;T. Nakamoto, M. Hanaya, M. Katada, K. Endo, S. Kitagawa, H. Sano, *Inorg.Chem*., **1997**, *36*, 4347.
15 T. Sato, K. Ishisita, M. Katada, H. Sano, Y. Aratono, C. Segawa, M. Saeki, *Chem. Lett.*, **1991**, 403;T. Sato, F. Ambe, K. Endo, M. Katada, H. Maeda, T. Nakamoto, H. Sano, *J. Am. Chem. Soc*., **1996**, *118,* 3450.
16 R. Wu, M. Poyraz, F. E. Sowrey, C. E. Anson, S. Wocadlo, A. K. Powell, U. A. Jayasooriya, R. D. Cannon, T. Nakamoto, M. Katada, H. Sano, *Inorg. Chem*., **1998**, *37*, 1913.
17 F. E Sowrey, C. Tilford, S. Wocadlo, C. E. Anson, A.K. Powell, S. M. Bennington, W. Montfrooij, U. A. Jayasooriya, R. D. Cannon, *J. Chem. Soc. Dalton Trans*., **2001**, 8620.
18 M. Ito, S. Onaka, H. Ebisu, M. Arakawa, Y. Yamada, T. Yoshida, *Inorg. Chim. Acta*, **2003**, *353*, 51.
19 Y. Sakai, S. Onaka, M. Takahashi, R. Ogiso, T. Takayama, T. Nakamoto, *Hyperfine Interact.*, **2012**, *205*, 1.
20 T. Sunahara, S. Onaka, M. Ito, H. Imai, K. Inoue, T. Ozeki, *Eur. J. Inorg. Chem.*, **2004**, 4882.
21 The structure of this manganese analogue has not yet been published.[18] The crystal data are as follows; $a = b$ =13.696(5) Å, c = 20.981(8) Å, $\gamma = 120^{\circ}$, Z = 2 at 298 K. The Mn-O(center) distance is 1.932(5) Å, which corresponds to detrapped Mn-O distances.
22 S. Matsubara, M. Katada, K. Sato, I. Motoyama, and H. Sano; J. de Phys., **40**, C2-363 (1979)
23 The Debye temperatures estimated here from Mössbauer data are those probed by ^{57}Fe locally. It is interesting to compare these "local" Debye temperatures with "total" Debye temperatures obtained by other methods, giving informations on the effective mass *M.*
24 "Supramolecular Materials and Technologies" ed. By D. N. Reinhoudt, J. Wiley, **4**, 1994.
25 "Transition Metals in Supramolecular Chemistry" ed. by L. Fabbrizziand A. Poggi, NATO ASI Sereis, **448**, 1994.
26 T. Umehara, N. Yanai, S. Kitagawa, *Chem. Soc. Rev*., 2009, **38**, 1228; S. Horike, S. Shimomura, S. Kitagawa, *Nature Chemistry*, 2009, **1**, 695.
27 M. Yoshizawa, J. K. Klosterman, M. Fujita, *Angew. Chem. Int. Ed*., 2009, **48**, 3418; J. K. Klosterman, Y. Yamauchi, M. Fujita, *Chem. Soc. Rev*., 2009, **38,** 1714; V. Maurizot, M. Yoshizawa, M. Kawano, M. Fujita, *Dalton Trans*., 2006, 2750.
28 Halogen analyses were made by ion chromatography. Cl analysis is suspected to be interfered by excess amount of F in **1**.
29 A. Altomare, G. Cascarano, C. Giacovazzo, A. Guagliardi, M. C. Burla, G. Polidori and M. Camalli, *J. Appl. Crystallogr*., **1994**, *27*, 435.
30 G. M. Sheldrick, *Acta Crystallogr.,Sect. A*, **2008**, *64*, 112.
31 L. Farrugia, *J. Appl. Crystallogr*., **2012**, *45*, 849.
32 K. Brandenburg, *Crystal Impact Gbr*, Postfach 1251, 53002 Bonn, Germany, 2012

Graphic content

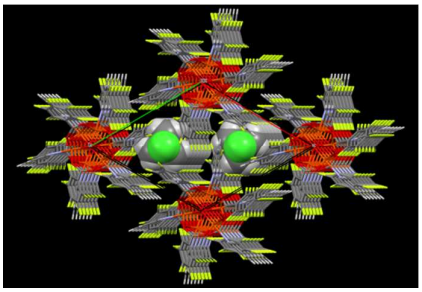

CH_2Cl_2 molecules trapped in the intermolecular nano-channels of the $Fe_3O(C_6F_5CO_2)_6(py)_3$ crystal